Evidence for universal flow and characteristics of early time thermalization in a scalar field model for heavy ion collisions

Margaret E. Carrington,[1,2] Wade N. Cowie,[3,2] Gabor Kunstatter,[4,5,2] and Christopher D. Phillips[1]

[1]*Department of Physics, Brandon University, Brandon, Manitoba R7A 6A9, Canada*
[2]*Winnipeg Institute for Theoretical Physics, Winnipeg, Manitoba, Canada*
[3]*Department of Physics, University of Manitoba, Winnipeg, Manitoba R3T 2N2, Canada*
[4]*Department of Physics, University of Winnipeg, Winnipeg, Manitoba R3M 2E9, Canada*
[5]*Department of Physics, Simon Fraser University, Burnaby, British Columbia V5A 1S6, Canada*

(Received 21 April 2024; accepted 18 July 2024; published 12 September 2024)

We study numerically the evolution of an expanding strongly self-coupled real scalar field. We use a conformally invariant action that gives a traceless energy-momentum tensor and is better suited to model the early time behavior of a system such as QCD, whose action is also conformally invariant. We consider asymmetric initial conditions and observe that when the system is initialized with nonzero spatial eccentricity, the eccentricity decreases and the elliptic flow coefficient increases. This behavior is characteristic of a hydrodynamic system in which pressure gradients are converted into fluid velocities, and therefore spatial anisotropy decreases while momentum anisotropy is generated. We look at a measure of transverse pressure asymmetry that has been shown to behave similarly to the elliptic flow coefficient in hydrodynamic systems and show that in our system their behavior is strikingly similar. We show that the derivative of the transverse velocity is proportional to the gradient of the energy in Milne coordinates and argue that this result means that transverse velocity initially develops in the same way that it does in hydrodynamic systems. We conclude that some aspects of the early onset of hydrodynamic behavior that has been observed in quark-gluon plasmas are seen in our numerical simulation of strongly coupled scalar fields.

DOI: 10.1103/PhysRevD.110.056020

I. INTRODUCTION

The quark-gluon plasma (QGP) has been observed experimentally to be well described by hydrodynamics at very early times (1 fm/c $\sim 3 \times 10^{-24}$ seconds) after formation. The successes of hydrodynamic modeling in describing heavy ion collision data motivates the development of a qualitative and quantitative understanding of the microscopic processes that connect an initial state of two Lorentz-contracted atomic nuclei with a hydrodynamic droplet of strongly coupled QGP in local thermodynamic equilibrium. This has been a subject of intense study over the past decade; for reviews, see Refs. [1–3]. In this work we take steps towards a full field theoretic approach which is extremely difficult in full quantum chromodynamics (QCD). We follow the approach of Refs. [4–6] [Dusling-Epelbaum-Gelis-Venugopalan (DEGV)] and use a simpler theory that has some properties in common with QCD but is nonetheless considerably more tractable. We consider a real, self-interacting scalar field in four spacetime dimensions. Like QCD, this theory is scale invariant and exhibits secular divergences in its perturbative solutions. These secular divergences are due to instabilities in the classical solutions. This system of scalar fields is therefore in some ways similar to the system of soft gauge fields produced in a heavy ion collision and called glasma [7].

DEGV used what is called the classical statistical approximation to resum the fastest growing divergences in this theory at each order in perturbation theory and showed that the scalar field system isotropizes when this resummation is performed [6]. The only observables considered were the energy and longitudinal/transverse pressures of the system, and it was found that the difference between the resummed longitudinal and transverse pressures tends towards zero. In a previous paper [8] we used the classical statistical approximation to study angular momentum in a system of expanding scalar fields. Some issues with the classical statistical approximation are discussed in [9,10]. A completely different technique to resum the dominant contributions based on a two-particle irreducible effective action approach can be found in [11].

In this paper we study the extent to which an expanding system of scalar fields behaves hydrodynamically, and how hydrodynamic behavior develops with time. We start with a

somewhat different theory than DEGV, one that we claim more closely models gluon behavior without losing the inherent simplicity of a real scalar field. Specifically, we consider a real scalar that is nonminimally coupled to the background geometry so as to produce a conformally invariant action, i.e., one that is invariant up to a total derivative under local scale transformations as well as global ones. This action produces a classical energy momentum tensor (EMT) that is manifestly symmetric, conserved, and traceless on-shell without altering the equations of motion on a Minkowski background. The theory therefore shares with QCD its conformal symmetry and the resulting tracelessness of the EMT. In the rest of this paper we refer to the EMT obtained from the nonminimally coupled conformally invariant action as the conformal EMT. The conformal and canonical EMTs are almost indistinguishable at late times[1] but at early times some components of the canonical EMT are characterized by rapid fluctuations that are absent in the conformal EMT.

We use the conformal EMT to study some observables that are related to the transverse asymmetry of the system of fields. Transverse asymmetry has been studied for many years in the context of quark-gluon plasmas. In a relativistic noncentral collision there is an initial spatial asymmetry that rapidly decreases with time, which means anisotropic transverse momentum can develop only at very early times. Since anisotropic flow is sensitive to the system's properties very early in its evolution, it can provide direct information about the early stages of the system. We find that if our system of scalar fields is initialized with spatial asymmetry, the asymmetry is transmitted into the momentum field. This behavior mimics what is seen in heavy ion collisions and is commonly considered an indication of the onset of some kind of hydrodynamic behavior. We also look at a measure of transverse pressure asymmetry that has been shown to behave similarly to the elliptic flow coefficient in quark-gluon plasmas. We show that in our system the behavior of these two quantities is qualitatively similar. Finally we investigate a proposal [12] that, under very general conditions, the derivative of the transverse velocity will be proportional to the gradient of the energy, and discuss the significance of the result.

This paper is organized as follows. In Sec. II we discuss the classical theory and the definition of the EMT. In Sec. III we describe the resummation method and give some details of the numerical procedure. We explain how the discretization of the equations is done, and our choice of boundary conditions and initial conditions. In Sec. IV we discuss how the energy density and the transverse and longitudinal pressures are obtained from the EMT. We derive some equations that characterize the hydrodynamic behavior of the system, and we define functions that measure the eccentricity, elliptic flow, and transverse pressure asymmetry of the system. In Sec. V we present our results and Sec. VI concludes with a summary and some observations. Some useful equations are collected in the Appendix.

Throughout this paper the spacetime is taken to be Riemannian with signature $(+,-,-,-)$. In addition to Minkowski coordinates (t,z,x,y) we will also use Milne coordinates (τ,η,x,y), where τ is the Bjorken time and η is spacetime rapidity. We choose units such that $c=k_B=\hbar=1$, where c is the speed of light in vacuum, k_B is the Boltzmann constant, and $\hbar$ is the Planck constant divided by 2π.

II. THE CLASSICAL THEORY

A. Canonical EMT

The Lagrangian density used by DEGV is that of a massless real scalar field[2]:

$$\mathcal{L}=\frac{1}{2}\nabla^\mu\varphi\nabla_\mu\varphi-V \quad \text{with} \quad V=\frac{g^2}{4!}\varphi^4. \tag{1}$$

The equation of motion is

$$\nabla_\mu\nabla^\mu\varphi+\frac{g^2}{3!}\varphi^3=0\rightarrow\varphi\Box\varphi+4V=0. \tag{2}$$

The canonical EMT is

$$\begin{aligned}T^{\mu\nu}_{\text{can}}&=\frac{\delta\mathcal{L}}{\delta(\nabla_\mu\varphi)}\nabla^\nu\varphi-g^{\mu\nu}\mathcal{L}\\&=\nabla^\mu\phi\nabla^\nu\phi-g^{\mu\nu}\left[\frac{1}{2}\nabla^\alpha\phi\nabla_\alpha\phi-\frac{g^2}{4!}\phi^4\right].\end{aligned} \tag{3}$$

Its divergence is

$$\begin{aligned}\nabla_\mu T^{\mu\nu}_{\text{can}}&=(\Box\varphi)(\nabla^\nu\varphi)+(\nabla_\mu)(\nabla^\mu\nabla^\nu\varphi)-g^{\mu\nu}(\nabla_\alpha\varphi)(\nabla_\mu\nabla^\alpha\varphi)\\&\quad+g^{\mu\nu}\frac{g^2}{3!}\varphi^3\nabla_\mu\varphi\\&=(\Box\varphi)(\nabla^\nu\varphi)+\frac{g^2}{3!}\varphi^3\nabla^\nu\varphi=0\end{aligned} \tag{4}$$

where we used the equation of motion in the last line. The conservation law (4) implies the conservation on shell of the momentum four-vector defined by

$$\mathcal{P}^\mu=\int d^3x\sqrt{-g}T^{\mu0} \tag{5}$$

[1]Time is measured in units of the transverse coordinate lattice spacing.

[2]We write everything covariantly since this will be useful when we switch to Milne coordinates, which are related to Minkowski coordinates by a nonlinear coordinate transformation.

provided the metric does not explicitly depend on the spacetime coordinates[3] and the fields vanish on the boundaries.

The trace of the canonical EMT is

$$T^{\mu}_{\mathrm{can}\mu} = -\nabla_\mu\varphi\nabla^\mu\varphi + 4V = -\nabla_\mu\varphi\nabla^\mu\varphi - \varphi\Box\varphi = -\nabla_\mu(\varphi\nabla^\mu\varphi) \tag{6}$$

using the equation of motion in the last step. The canonical EMT is therefore not traceless. The QCD canonical EMT is also not traceless, and additionally it is not symmetric or gauge invariant. These problems can be remedied using several different methods (see [13] for a detailed discussion). In this work we define the EMT from a conformally invariant scalar field action. It is manifestly traceless due to the conformal invariance of the action. It is also conserved and symmetric.

B. Covariant EMT

In this section, we derive the conformal EMT for the real massless scalar field that, like the EMT used for QCD, is traceless. In Sec. IV A we explain further why the definition given in this section is a better choice for our purposes.

The real scalar field Lagrangian (1) is invariant under constant scale transformations in which the spacetime metric and scalar field transform as

$$g_{\mu\nu} \to \Omega g_{\mu\nu} \quad \text{and} \quad \varphi \to \Omega^{-\frac{1}{2}}\varphi \tag{7}$$

with constant Ω. It is, however, not invariant under local scale transformations (i.e., conformal transformations) for which $\Omega = \Omega(x)$ is an arbitrary function of the spacetime coordinates that goes to unity on the boundaries. The Lagrangian density of QCD is conformally invariant and to incorporate as many of the fundamental properties of QCD into our theory as possible, we start with a conformally invariant theory. The Lagrangian density is [14]

$$\mathcal{L}_\xi = \frac{1}{2}\sqrt{-g}(g^{\mu\nu}\nabla_\mu\nabla_\nu\varphi - \xi R\varphi^2 - V) \tag{8}$$

where R is the scalar curvature of the spacetime. The choice $\xi = 0$ gives the original Lagrangian (1) and is called the minimally coupled theory. In four dimensions with $\xi = 1/6$ the Lagrange density changes by a total derivative under the transformation (7) with nonconstant $\Omega(x)$.

The equation of motion for the scalar field is

$$\left(\Box + \frac{R}{6} + \frac{g^2}{3!}\varphi^2\right)\varphi = 0. \tag{9}$$

[3]This condition is not satisfied in Milne coordinates.

The metric is treated as a fixed background field and is therefore not dynamical. When evaluated on a Minkowski background (zero curvature), Eq. (9) reduces to the equation of motion (1) of the original theory.

The fact that the action is invariant under a general coordinate transformation $x^\mu \to x'^\mu - \epsilon^\mu(x)$ leads to the definition of a conserved, symmetric EMT [14]

$$T^{\mu\nu} = -\frac{2}{\sqrt{-g}}\frac{\delta\mathcal{L}}{\delta g_{\mu\nu}}. \tag{10}$$

One advantage of the definition in (10) is that the tensor $T^{\mu\nu}$ is always symmetric and preserves the symmetries of the Lagrangian density. This is not necessarily true for the definition in Eq. (3). The resulting EMT for the Lagrange density in (8) is

$$T^{\mu\nu} = \nabla^\mu\phi\nabla^\nu\phi - g^{\mu\nu}\left[\frac{1}{2}\nabla^\alpha\phi\nabla_\alpha\phi - \frac{g^2}{4!}\phi^4\right] + \frac{1}{6}[g^{\mu\nu}\Box - \nabla^\mu\nabla^\nu]\varphi^2 - \frac{1}{6}\left(R^{\mu\nu} - \frac{1}{2}g^{\mu\nu}R\right)\varphi^2. \tag{11}$$

It is straightforward to verify that $T^{\mu\nu}$ is traceless and divergenceless in four dimensions. In flat spacetime where $R = 0$ we can write this result in the form

$$T^{\mu\nu} = T^{\mu\nu}_{\mathrm{can}} + T^{\mu\nu}_{\mathrm{ex}}, \qquad T^{\mu\nu}_{\mathrm{ex}} = \frac{1}{6}[g^{\mu\nu}\Box - \nabla^\mu\nabla^\nu]\varphi^2 \tag{12}$$

where $T^{\mu\nu}_{\mathrm{can}}$ is the canonical EMT (3).

C. Milne coordinates

Milne coordinates are defined as

$$\tau = \sqrt{t^2 - z^2} \quad \text{and} \quad \eta = \frac{1}{2}\ln\left(\frac{t+z}{t-z}\right) \tag{13}$$

which gives $t = \tau\cosh(\eta)$ and $z = \tau\sinh(\eta)$. The metric is

$$g = (1, -\tau^2, -1, -1)_{\mathrm{diag}}. \tag{14}$$

The coordinate η is called the rapidity and depends only on the slope $v_z = \frac{z}{t}$. A change of η corresponds to a boost by velocity v_z. It is therefore also referred to as a boost coordinate. Surfaces of constant η represent timelike surfaces moving away from the origin at constant velocity and a box with boundaries at fixed η expands in the z direction with time. In this sense Milne coordinates mimic the kinematics of a high energy collision. In our notation a "dot" indicates a derivative with respect to τ, and $\vec{\nabla}_\perp$ is the transverse gradient operator. The Riemann tensor and the Ricci scalar are both zero and therefore the equation of

motion (9) is the same as the one obtained from the minimally coupled theory (2). In Milne coordinates it takes the form

$$\ddot{\phi}(\tau,\eta,\vec{x}_\perp)+\frac{1}{\tau}\dot{\phi}-\frac{1}{\tau^2}\partial_\eta^2\phi-\nabla_\perp^2\phi+\frac{g^2}{6}\phi^3=0. \quad (15)$$

In the Appendix we write all components of the two EMTs (3) and (11) in Milne coordinates.

III. RESUMMATION OF QUANTUM FLUCTUATIONS

Observables in the scalar theory exhibit secular divergences at next-to-leading order if they are calculated in a loop expansion. These divergences originate from instabilities of the classical solutions. The problem can be cured using the classical statistical approximation, which amounts to averaging over a Gaussian ensemble of initial conditions [4,6]. This procedure implements a resummation scheme that collects the leading secular terms at each order of an expansion in the coupling constant.[4] We briefly describe the structure of the calculation. Further details can be found in [6,8].

A. Fluctuations

We define an ensemble of initial fields at some small but nonzero[5] $\tau=\tau_0$ as the sum of a background field contribution, $\varphi(\tau_0,\vec{x}_\perp)$, and a fluctuation, $\alpha^{(\gamma)}(\tau_0,\eta,\vec{x}_\perp)$

$$\phi^{(\gamma)}(\tau_0,\eta,\vec{x}_\perp)=\varphi(\tau_0,\vec{x}_\perp)+\alpha^{(\gamma)}(\tau_0,\eta,\vec{x}_\perp). \quad (16)$$

The field $\phi^{(\gamma)}(\tau,\eta,\vec{x}_\perp)$ at finite proper time is obtained by solving Eq. (15) with the initial condition (16). We then obtain resummed values of observable quantities by averaging over the ensemble:

$$\langle O(\tau,\eta,x_\perp)\rangle=\frac{1}{N_\gamma}\sum_{\gamma=1}^{N_\gamma}O[\phi^{(\gamma)}(\tau,\eta,x_\perp)].$$

We explain below how the two terms in (16) are calculated and the meaning of the index γ.

The field $\varphi(\tau_0,\vec{x}_\perp)$ is constructed from solutions of the classical equation of motion (15) at τ_0. It is assumed independent of the spatial rapidity η. The motivation behind this assumption is the physical picture of a heavy ion collision in which the nuclei pass through each other without significant slowing. The resulting velocity distribution has a property called Bjorken boost invariance—which is that the longitudinal velocity v_z of frames locally comoving with the fluid is related to their spacetime position by $v_z=z/t$. A fluid with this velocity distribution will look the same in all longitudinally comoving fluid elements. We also assume that at very early times the dynamics of the system is dominated by expansion and we therefore drop the interaction term in the equation of motion for the purposes of determining $\varphi(\tau_0,\vec{x}_\perp)$. The resulting equation is linear in φ and separating variables we have that at fixed τ_0 the background field can be written as a sum over plane wave mode functions. The specific combinations of plane waves that we use are discussed in Sec. III C.

The fluctuation α that is added to the background field in Eq. (16) carries an index γ that indicates a Gaussian ensemble of N_γ initial fluctuations defined as

$$\alpha^{(\gamma)}(\tau_0,\eta,\vec{x}_\perp)=\int dK[c_K^{(\gamma)}a_K+c_K^{(\gamma)*}a_K^*] \quad (17)$$

where the index K labels the momentum variables $(\nu,\vec{k}_\perp)$ that are conjugate to the coordinate-space variables $(\eta,\vec{x}_\perp)$, respectively. The notation $c_K^{(\gamma)}$ denotes an element in a Gaussian distributed ensemble of N_γ random numbers, with variance

$$\langle c_K^* c_L\rangle \coloneqq \sum_{\gamma=1}^{N_\gamma}c_K^{(\gamma)*}c_L^{(\gamma)}=\frac{1}{2}\delta_{KL}. \quad (18)$$

The momentum space integration measure is $dK=d\nu d\vec{k}_\perp/(2\pi)^3$ and the delta function in Eq. (18) is defined so that $\int dK\delta_{KL}=1$. The initial mode functions $a_K\equiv a_{\nu\vec{k}_\perp}(\tau_0,\eta,\vec{x}_\perp)$ are obtained from the linearized equations of motion

$$\ddot{a}_K+\frac{1}{\tau}\dot{a}_K-\frac{1}{\tau^2}\partial_\eta^2 a_K-\Delta_\perp a_K+\frac{g^2}{2}\varphi^2(\tau_0,\vec{x}_\perp)a_K=0 \quad (19)$$

and normalized so that $\int dK(a_K,a_L)=1$ with

$$(a_K,a_L)=i\tau\int d\eta\int d^2\vec{x}_\perp(a_K^*\partial_\tau a_L-(\partial_\tau a_K^*)a_L). \quad (20)$$

Separating variables and performing the normalization one finds[6]

[4]The resulting EMT has an ultraviolet divergence corresponding to a vacuum contribution but this can be removed by repeating the calculation with the background field set to zero and subtracting the results. This vacuum subtraction has been done for all the calculations presented in this paper.

[5]The initial time τ_0 must be small in order to describe a system expanding from essentially zero volume ($z=0$ at $t=0$) but it cannot be exactly zero due to the coordinate singularity at $\tau=0$. One can check that the value chosen for this small initial time does not change the results at finite times.

[6]The time dependent part of the equation is second order and has two independent solutions. We use only the one that has positive frequency behavior at large times which is called the second Hankel function.

$$a_K \equiv a_{\nu\vec{k}_\perp}(\tau_0,\eta,\vec{x}_\perp) = \frac{1}{2}\sqrt{\pi}e^{\pi\nu/2}e^{i\nu\eta}\chi_{\vec{k}_\perp}(\vec{x}_\perp)H_{i\nu}(\lambda_{\vec{k}_\perp}\tau_0) \tag{21}$$

where the functions $\chi_{\vec{k}_\perp}(\vec{x}_\perp)$ are solutions of the eigenvalue equation

$$\left[-\Delta_\perp + \frac{g^2}{2}\varphi^2(\tau_0,\vec{x}_\perp)\right]\chi_{\vec{k}_\perp}(\vec{x}_\perp) = \lambda^2_{\vec{k}_\perp}\chi_{\vec{k}_\perp}(\vec{x}_\perp) \tag{22}$$

and the notation $H_{i\nu}$ indicates a Hankel function of the second kind (we omit the superscript (2) to simplify the notation). When $\tau \to 0$ the Hankel function oscillates like $e^{\pm i\tau\nu}$ and the derivative diverges. As explained at the beginning of this section, we start the evolution at a small positive time $\tau_0 = 10^{-2}$. To calculate the Hankel function at this initial time we use an asymptotic series to find it at the smallest time for which the series converges to the desired accuracy (numerically we truncate the series when successive terms are less than 10^{-9}), and then use adaptive fifth order Runge-Kutta to evolve it to the initial time τ_0.

B. Discretization

We discretize in both directions in the transverse plane with L grid points and lattice spacing set to one, which means we define all dimensionful quantities in terms of the transverse lattice grid spacing. This is made possible by the scale invariance of the theory, i.e., the only physical scale is set by the initial conditions. The rapidity variable η is discretized with N grid points and lattice spacing h. We consider a unit slice of rapidity with $\eta \in (-1/2, 1/2)$ and $h = 1/N$. The discretized version of Eq. (22) is

$$D_{ij;kl}\chi_{kl} = \lambda^2\chi_{ij} \tag{23}$$

with

$$\begin{aligned} D_{ij;kl} = {} & (4 + V''_{ij})\delta_{ik}\delta_{jl} - (\delta_{i+1\,k} + \delta_{i-1\,k})\delta_{jl} \\ & - \delta_{ik}(\delta_{j+1\,l} + \delta_{j-1\,l}). \end{aligned} \tag{24}$$

Since D is a rank 4 tensor with L^4 components, we obtain L eigenvalues λ^e with $e \in (1, L^2)$ and L^2 eigenfunctions χ^e_{ij} which are normalized $\sum_{ij}\chi^{*e}_{ij}\chi^{\bar{e}}_{ij} = L^2\delta^{e\bar{e}}$. To discretize the longitudinal variables we note that the constraint $\partial^2_\eta e^{i\nu\eta} = -\nu^2 e^{i\nu\eta}$ gives

$$\varepsilon_v := \nu = \frac{2}{h}\left|\sin\left(\frac{\pi v}{N}\right)\right| \tag{25}$$

and we replace $\nu \to \varepsilon_v$ in every factor $e^{\pi\nu/2}$. For the complex exponential we use $e^{i\nu\eta} \to e^{\frac{2\pi i v n}{N}}$ and the integral over ν becomes a sum over v using $\int d\nu/(2\pi) \to 1/(Nh)\sum_v^N$.

Combining these results we find the discretized versions of Eqs. (16), (18), and (21):

$$\begin{aligned} \alpha_{nij}(\tau) &= \frac{1}{NL^2h}\sum_{v=1}^{N}\sum_{p=1}^{L^2}[c_{vp}a^{vp}_{nij}(\tau) + \text{c.c.}] \\ a^{vp}_{nij}(\tau) &= \frac{1}{2}\sqrt{\pi}e^{\frac{2\pi i v n}{N}}\chi^p_{ij}e^{\pi\nu/2}H_{i\nu}(\lambda_{\vec{k}_\perp}\tau) \\ \langle c_{ve}c^*_{u\tilde{e}}\rangle &= \frac{1}{2}NL^2h\delta_{vu}\delta_{e\tilde{e}}. \end{aligned} \tag{26}$$

To verify that the discretization is done correctly we have checked the discretized version of the normalization condition (20).

We use periodic boundary conditions which means that the indices (i, j) that correspond to the transverse spatial coordinates are defined modulo L, and the index n for the rapidity is modulo N. The boundary conditions satisfy the self-adjointness condition

$$\begin{aligned} \nabla_F\phi(x) &\equiv \phi(i+1) - \phi(i) \\ \nabla_B\phi(x) &\equiv \phi(i) - \phi(i-1) \\ \sum_i f(i)(\nabla_F g(i)) &= -\sum_i (\nabla_B f(i))g(i). \end{aligned}$$

We use forward derivatives, defined as $\partial_x f(x) \to f(i+1) - f(i)$, so that the integral of a total derivative term like the last term in Eq. (6) will be zero.

C. Initialization

As explained in Sec. III A, the initial background field $\varphi(\tau_0,\vec{x}_\perp)$ can be written as a sum of plane wave mode functions of the form $\cos(\vec{k}_\perp\cdot\vec{x}_\perp)$. In this section we discuss how to choose these functions and construct the sum. Ideally we would like to consider initializations that correspond to collisions of sources with a specified radius colliding with a specified impact parameter, and we could do this by constructing a wave packet of transverse plane waves that corresponds to a collision with some specific geometry.[7] This calculation is considerably more difficult than what has been done so far with the method of DEGV. For the purposes of studying the isotropization of the longitudinal and transverse pressures, it is sufficient to consider a classical background field that consists of only one mode, which corresponds to sources with constant

[7]Since the sources that describe the colliding projectiles have support only on the light cone (15), they do not directly drive the field evolution, but instead provide information on how to construct this wave-packet. In a color glass condensate (CGC) description of a heavy ion collision, the background field would contain a distribution of momentum modes up to the saturation momentum.

surface charge densities with infinite spatial extent.[8] In this paper we restrict ourselves to the consideration of several different initializations involving asymmetric combinations of two transverse plane waves.

The initial condition that we use for the background field is

$$\varphi(\tau_0, \vec{x}_\perp) = \varphi_0(\cos(k_x x + k_y y) + A\cos(k_y y)) \tag{27}$$

and the time derivative of the background field at $\tau = \tau_0$ is set to zero (numerically 10^{-3}). The momenta k_x and k_y are chosen to take a range of values below the largest lattice eigenvalue, which is $\sqrt{8}$. The reader will note that our initial classical field is not always periodic and therefore does not respect our boundary conditions. The reason is that we want to avoid problems that may arise when resonant modes are considered, which in the present model would correspond to the normal modes of the finite spatial lattice. For a large enough lattice all modes are effectively periodic and it is therefore expected that the precise form of the initial boundary conditions is not important.

IV. PHYSICAL OBSERVABLES

A. Canonical and conformal EMTs in Minkowski and Milne coordinates

The EMT is conserved

$$\nabla_\mu T^{\mu\nu} = \partial_\mu T^{\mu\nu} + \Gamma^\mu_{\mu\sigma} T^{\sigma\nu} + \Gamma^\nu_{\mu\sigma} T^{\mu\sigma} = 0 \tag{28}$$

which means that there is a momentum four-vector

$$\mathcal{P}^\nu = \int d\sigma_\mu T^{\mu\nu}, \tag{29}$$

where $d\sigma_\mu$ is an element of a spacelike surface σ, whose components are conserved by the time evolution provided that the metric contains no explicit dependence on the coordinates x^μ and the fields vanish on the boundaries of σ. This can be seen by noting that in Minkowski coordinates the integral of the $\nu = 0$ component of the conservation law (28) takes the form

$$\int d^3x \frac{\partial}{\partial t} T^{00} = -\int d^3x (\partial_x T^{x0} + \partial_y T^{y0} + \partial_z T^{z0}). \tag{30}$$

The right side is the integral of a total derivative so assuming the fields vanish at spatial infinity one finds that the energy defined as $E = \int d^3x T^{00}$ is conserved ($dE/dt = 0$).

In Milne coordinates the situation is more complicated due to the τ dependence of the metric so that $\int d^3x \sqrt{-g} T^{00}$ integrated along a surface of constant τ is not, in general, conserved, even for an isolated system. In Milne coordinates the only nonzero components of the connection are $\Gamma^0_{\eta\eta} = \tau$ and $\Gamma^\eta_{0\eta} = \Gamma^\eta_{\eta 0} = 1/\tau$. The $\nu = 0$ component of the divergence equation (28) gives

$$\frac{\partial T^{00}}{\partial \tau} = -\partial_\eta T^{\eta 0} - \frac{1}{\tau} T^{00} - \tau T^{\eta\eta} - \partial_x T^{x0} - \partial_y T^{y0}. \tag{31}$$

We define the energy density and longitudinal and transverse pressures in terms of the EMT in Milne coordinates as

$$\begin{aligned} \mathcal{E} &= \langle T^{00} \rangle \\ p_L &= \tau^2 \langle T^{\eta\eta} \rangle \\ p_T &= \frac{1}{2} \langle T^{xx} + T^{yy} \rangle \end{aligned} \tag{32}$$

where the angle brackets indicate an average over rapidity and the transverse coordinates. Since the average of a total derivative vanishes, Eq. (31) gives

$$\frac{\partial \mathcal{E}}{\partial \tau} = -\frac{1}{\tau}(\mathcal{E} + p_L). \tag{33}$$

We note that when the EMT is written in Milne coordinates, T^{00} does not correspond to the physical energy density as measured in the lab frame except at zero rapidity. In our calculation we include only a narrow slice of rapidity centered around midrapidity ($\eta = 0$). The motivation is that we are trying to model the gluon fields produced in a relativistic collision of heavy ions for which the system of fields is largely rapidity independent at midrapidity. The definitions in (32) also involve an average over this thin slice of rapidity. We therefore take the energy density and pressures as defined in (32) as the physically relevant ones.

Now we address the fact that the canonical and conformal EMTs are not the same even when they are calculated in the same coordinate system. Equation (A4) shows that the difference between the two EMTs, for all components, is a sum of terms that are either a total derivative in transverse coordinates, a total derivative in rapidity, or contain the product of the field and its time derivative (below we call the product $\phi\dot{\phi}$ a decoherence factor). As explained previously, the total derivative terms do not affect the bulk properties of the medium because they give zero when they are averaged. The important point to understand when comparing the two EMTs is that the decoherence factor goes rapidly to zero at very early times. At $\tau = \tau_0$ we start with a fairly narrow Gaussian distribution of initial conditions centered on the chosen initial values $\varphi(\tau_0, \vec{x}_\perp)$ and $\dot{\varphi}(\tau_0, \vec{x}_\perp)$. Each initial condition evolves independently using the equation of motion so that after some characteristic decoherence time the ensemble average of the product $\phi\dot{\phi}$ goes to zero. This means that the integrated EMT in (3) is the same as the conformal form (10) except at very early times. If we only

[8] In the CGC approach this is called the McLerran-Venugopalan model.

wanted to study late time properties of the system, like transverse-longitudinal pressure isotropization, both EMTs would be equally good. Since we are particularly interested in early time behavior however, it is important to know which formalism is better for our purposes.

To understand this we consider the trace of the two EMTs. The trace of the conformal EMT is zero by construction. The trace of the canonical EMT is

$$T^{\mu}_{\mu} = -\nabla^{\mu}(\phi\partial_{\mu}\phi) = -\frac{d}{d\tau}(\varphi\dot{\varphi}) - \frac{\varphi\dot{\varphi}}{\tau} + \vec{\nabla}_{\perp}\cdot(\varphi\vec{\nabla}_{\perp}\varphi). \quad (34)$$

This expression has terms that are proportional to the decoherence factor and its derivative, in addition to total derivatives, which means that the trace of the averaged canonical EMT is not zero at early times. We are interested in assessing the extent to which our system of fields behaves hydrodynamically, and the traditional formulation of hydrodynamics based on the assumption of local equilibrium assumes a traceless EMT (see Sec. IV C). This suggests that we want to work with the conformal definition of the EMT. Furthermore, in Sec. V we present some results that show that at early times the time dependence of the canonical EMT is characterized by rapid oscillations created by decoherence terms. These oscillations disappear at larger times but make it impossible to study early time dynamics. They are not present when the conformal EMT is used.

Finally we make the formal argument that we should work with a conformally invariant theory since we hope to use the scalar system to understand some properties of glasma.

B. Spatial and momentum asymmetries

A correlation between initial spatial transverse asymmetry and azimuthal asymmetry in the momentum field is generally considered characteristic of the onset of hydrodynamic behavior. Physically the idea is that if pressure gradients are converted into fluid velocities, then momentum anisotropy will grow as the spatial anisotropy decreases. Spatial deviations from azimuthal symmetry can be characterized with the quantity

$$\varepsilon = -\frac{\int d^2x_{\perp}\left(\frac{x^2-y^2}{\sqrt{x^2+y^2}}\right)T^{00}}{\int d^2x_{\perp}\sqrt{x^2+y^2}T^{00}} \quad (35)$$

where we have used $\vec{x}_{\perp} = (x, y)$. We note that several definitions of the spatial eccentricity are in common use; see the reviews [15,16]. Our definition is similar to that of Refs. [17,18] but slightly modified to make comparison with the elliptic flow coefficient more direct [see Eq. (36)].

In a system of fields, momentum anisotropy can be described by an elliptic flow coefficient defined as [19]

$$v_2 = \frac{\int d^2x_{\perp}\left(\frac{(p^x)^2-(p^y)^2}{\sqrt{(p^x)^2+(p^y)^2}}\right)}{\int d^2x_{\perp}\sqrt{(p^x)^2+(p^y)^2}} \quad (36)$$

where $p^x = T^{0x}$ and $p^y = T^{0y}$. A different quantity that is commonly calculated in heavy ion physics is the transverse pressure anisotropy defined

$$A_{xy} = \frac{\int d^2\vec{x}_{\perp}(T^{xx} - T^{yy})}{\int d^2\vec{x}_{\perp}(T^{yy} + T^{xx})}. \quad (37)$$

Hydrodynamic calculations show that A_{xy} is closely related to the elliptic flow coefficient of produced particles [17] and the transverse pressure anisotropy has been used extensively in the literature to characterize momentum anisotropy [20,21].

We caution the reader that the definitions of v_2 and A_{xy} that we use are not directly related to what is normally measured in heavy ion collisions, where one looks at the momentum distribution of produced particles. We consider a system of fields only. In a physical theory (if we had done a QCD calculation instead of using ϕ^4 theory) we expect the fields to convert into particles (hadrons) as the system expands and cools. However, the asymmetry of the initial system of fields could be significantly washed out by the thermal motion of the final state particles. For this reason the field definitions of v_2 and A_{xy} that we use are certainly not equivalent to the experimentally relevant definitions that measure the asymmetry in the momenta of produced particles. Our goal is only to investigate if a similar correlation between the two quantities is found for a system of fields.

C. Universal flow

The authors of Ref. [12] derived an equation that describes the way transverse flow develops for any system for which the longitudinal flow is boost invariant, the EMT is traceless, and the anisotropy of the spatial components of the EMT depends more strongly on τ than on the transverse coordinates at early times. They showed that the equation is well satisfied for three different models that have very different asymmetries between the transverse and longitudinal pressures. In our calculation the condition of boost invariance is satisfied by construction, the EMT is always traceless using the conformal definition, and the third condition of [12] is well satisfied for the initializations we use.

We define the x component of a velocity and an effective acceleration

$$V_x = \frac{T^{0x}}{T^{00}}$$
$$\alpha = \frac{\partial V_x}{\partial \tau} = \frac{\partial}{\partial \tau}\left(\frac{T^{0x}}{T^{00}}\right) = \frac{\partial_\tau T^{0x}}{T^{00}} - \frac{T^{0x}}{T^{00}}\frac{\partial_\tau T^{00}}{T^{00}}. \quad (38)$$

We can rewrite this in a more convenient form as follows. The zeroth component of the equation $\nabla_\mu T^{\mu\nu}$ in Milne coordinates is given in Eq. (31). The x component is

$$\frac{\partial T^{0x}}{\partial \tau} = -\frac{1}{\tau}T^{0x} - \partial_x T^{xx} - \partial_y T^{yx} \quad (39)$$

where we have dropped the derivative with respect to η since we are interested in a system that is at least approximately boost invariant. We will assume that T^{yx} is small and set it to zero. We rewrite α using Eqs. (31) and (39) to obtain

$$\begin{aligned} T^{00}\alpha &= \partial_\tau T^{0x} - \frac{T^{0x}}{T^{00}}\partial_\tau T^{00} \\ &= -\left(\frac{1}{\tau}T^{0x} + \partial_x T^{xx}\right) \\ &\quad + \frac{T^{0x}}{T^{00}}\left(\frac{1}{\tau}T^{00} + \tau T^{\eta\eta} + \partial_x T^{x0} + \partial_y T^{y0}\right). \end{aligned} \quad (40)$$

We assume that at early times the field ϕ has a power series expansion in τ and define

$$\phi = \sum_{i=0} \phi_{2i}\tau^{2i} \quad (41)$$

where only even powers of τ are included because the equation of motion does not allow solutions with odd powers with our initial conditions. From the explicit expressions for the components of the EMT (A3), (A4) we see that the diagonal components are series with only even powers of τ and both T^{x0} and T^{y0} have only odd powers. We define $T^{00} = T^{00}_0 + T^{00}_2\tau^2 + \cdots$ where the subscript indicates the power of τ associated with each coefficient and similarly for each component of the EMT.

We write $\alpha = \alpha_0 + \cdots$ where $\alpha_0 = T^{0x}_1/T^{00}_0$ and keep terms in (40) to order τ^0 which gives

$$T^{0x}_1 = -\partial_x T^{xx}_0 - T^{0x}_1 + \frac{T^{0x}_1}{T^{00}_0}(T^{00}_0 + T^{\eta\eta}_{-2}). \quad (42)$$

Rearranging we have

$$T^{0x}_1(T^{00}_0 - T^{\eta\eta}_{-2}) = -T^{00}_0\partial_x T^{xx}_0. \quad (43)$$

The condition that the trace is zero, to zeroth order in τ, is $T^{00}_0 - T^{\eta\eta}_{-2} - T^{xx} - T^{yy} = 0$. Equation (43) therefore takes the form

$$T^{0x}_1 = -\frac{T^{00}_0}{T^{xx}_0 + T^{yy}_0}\partial_x T^{xx}_0. \quad (44)$$

We assume that at early times $T^{xx} \approx T^{yy}$ and that T^{00}/T^{xx} is approximately independent of $\vec{x}_\perp$. Using these assumptions and multiplying by τ, Eq. (44) gives

$$T^{0x} = -\frac{\tau}{2}\partial_x T^{00} + \mathcal{O}(\tau^2) \quad (45)$$

or equivalently

$$\frac{\partial v_x}{\partial \tau} = -\frac{1}{2}\frac{\partial_x T^{00}}{T^{00}} + \mathcal{O}(\tau^2). \quad (46)$$

This result tells us that at early times the impulse to the transverse collective flow is connected to the gradient of the energy density. It means that different systems with the same energy density but very different pressures, ranging from hydrodynamic $p_T = p_L = \mathcal{E}/3$ to systems with highly asymmetric initial pressures like ours, will develop transverse flow in the same way. In Sec. V we show that (45) is well satisfied in our calculation, at early times.

For comparison we discuss how (45) can be derived for a system governed by hydrodynamics. The hydrodynamic definition of the EMT in Minkowski coordinates is

$$T^{\mu\nu}_{\text{hydro}} = (\epsilon + p)u^\mu u^\nu - p g^{\mu\nu} \quad (47)$$

where ϵ is the energy density, p is the thermodynamic pressure, and $u^\mu = \gamma(1, \vec{v})$ is the fluid velocity. The tracelessness of the EMT gives the equation of state $p = \epsilon/3$. If we assume that each velocity component can be written as a power series in t

$$v^i = v^i_0 + v^i_1 t + v^i_2 t^2 + \ldots \quad (48)$$

then at leading order we find

$$T^{0x} = -t\frac{\partial T^{xx}}{\partial x} + \mathcal{O}(t^2) \quad (49)$$

and since $T^{xx} = p = \epsilon/3$ we have

$$T^{0x} = -\frac{t}{3}\frac{\partial T^{00}}{\partial x} + \mathcal{O}(t^2). \quad (50)$$

The same calculation in two spatial dimensions gives

$$T^{x0} = -\frac{t}{2}\frac{\partial T^{00}}{\partial x} + \mathcal{O}(t^2) \quad (51)$$

which agrees with (45) at midrapidity.

The derivation of the flow equation in the first part of this section, and the two-dimensional hydrodynamic calculation presented above appear to be very different from

each other. One starts from an EMT derived from a field theory that describes the system on a microscopic level, and the other from a hydrodynamic model for the energy-momentum tensor. The assumptions used to derive Eq. (45) (tracelessness of the EMT, boost invariance, and weak transverse isotropy) are not obviously related to the existence of local thermal equilibrium. The fact that the flow equation obtained from our EMT has the same structure as a hydrodynamic flow equation is interesting and might be connected to the fact that other aspects of the behavior of the scalar system of fields that we study are hydrodynamiclike.

V. RESULTS

Our goal is to study how the system isotropizes. We are particularly interested in understanding the extent to which the system behaves hydrodynamically, and how hydrodynamic behavior develops with time. Unless stated otherwise, all calculations are done with $(N, L, N_\gamma) = (121, 41, 256)$. We have checked that results are not sensitive to these numbers. The initialization is specified by giving the values of (φ_0, A, k_x, k_y) that are used in Eq. (27). The coupling is $g = 4$ in all calculations. Because of computational constraints, we have not explored the dependence of our results on the value of g, but we mention that in [6] it was shown that the isotropization of longitudinal and transverse pressures is qualitatively similar for a wide range of couplings.

A. Trace of the canonical EMT and the energy conservation equation

The trace of the averaged canonical EMT is not zero, as shown in Eq. (6), but it goes rapidly to very small values as the system evolves because the decoherence factor goes to zero. In Fig. 1 we show the energy and the sum of the pressures for the canonical EMT. The blue curve, which shows the sum of the pressures, oscillates around the red curve, which shows the energy, until $\tau \approx 20$. At larger times the trace (the difference between the blue and red lines) is numerically very close to zero. For the conformal EMT the sum of the pressures and the energy are right on top of the canonical energy curve. The oscillations in the pressures from the canonical EMT are typical of the early time behavior and caused by the decoherence terms.

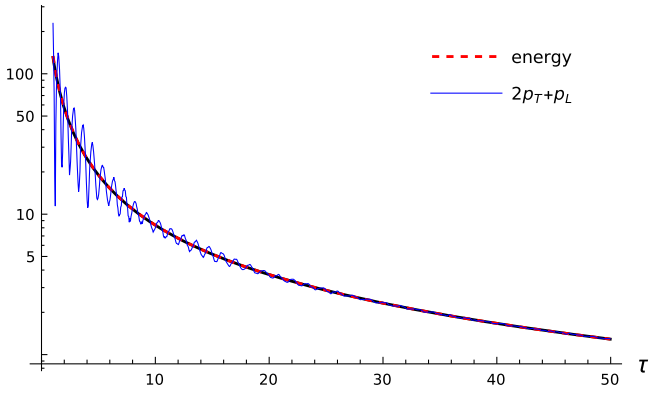

FIG. 1. The energy (red) and the sum $p_L + 2p_T$ (blue) for the canonical EMT. For the conformal EMT the sum of the pressures and the energy are right on top of the canonical energy curve. The calculation is done with $(\varphi_0, A) = (15, 0)$ and $k_x = k_y = 0.41$.

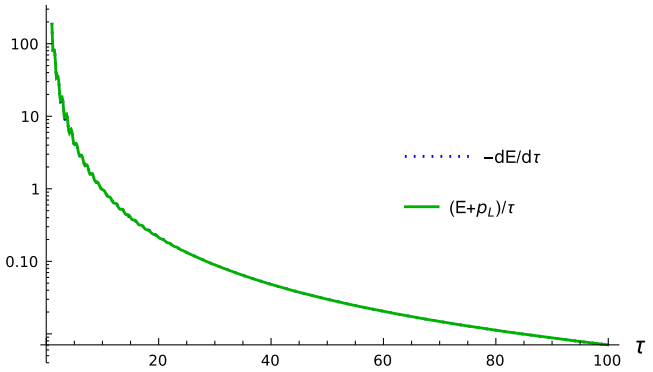

FIG. 2. The left and right sides of Eq. (52).

The energy conservation condition in Milne coordinates is given in Eq. (31). For a boost invariant system, and dropping the derivatives with respect to the transverse coordinates which average to zero using periodic boundary conditions, this equation has the form

$$\frac{\partial \mathcal{E}}{\partial \tau} = -\frac{\mathcal{E} + p_L}{\tau}. \tag{52}$$

Equation (52) shows that the time evolution of the energy density is related to the longitudinal pressure. Physically it means that the energy decreases due to longitudinal expansion. The equation comes from the conservation of energy and momentum and is not related to hydrodynamics. We have checked that it is satisfied numerically to very high accuracy in our calculation (see Fig. 2).

B. Transverse-Longitudinal isotropization

A simple way to study how the system comes to equilibrium is to see how closely it satisfies the isotropic equation of state: $p_L = p_T = \mathcal{E}/3$. This was studied by DEGV who showed that $(p_T - p_L)/\mathcal{E}$ decreases as a function of time. The result is important because it proves that the resummation method developed by DEGV is successful in capturing the dominant physics of the expanding plasma.

Figure 3 shows the transverse and longitudinal pressures normalized by the energy from the canonical EMT for two initializations that have the same initial field amplitude. The figure shows that the isotropization of the transverse and longitudinal pressures is not significantly affected when the second cosine is included in the initialization.

In Fig. 4 we show the transverse and longitudinal pressures normalized by the energy for the canonical

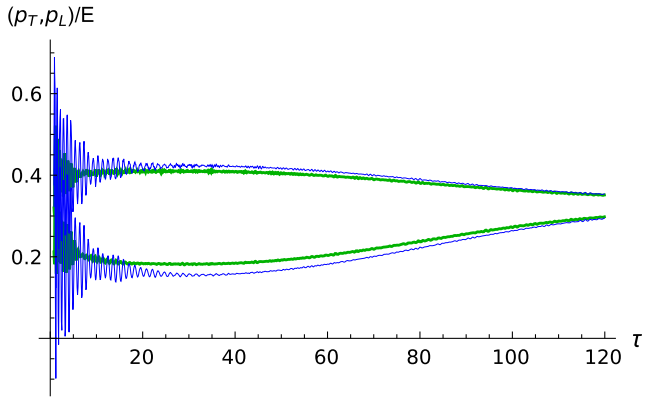

FIG. 3. The transverse and longitudinal pressures normalized by the energy from the canonical EMT for the initializations $(\varphi_0, A) = (15, 0)$ and $(\varphi_0, A) = (15/\sqrt{2}, 1)$. Both calculations are done with $k_x = k_y = 0.41$. In both cases the upper curves are $p_T/\mathcal{E}$ and the lower lines are $p_L/\mathcal{E}$.

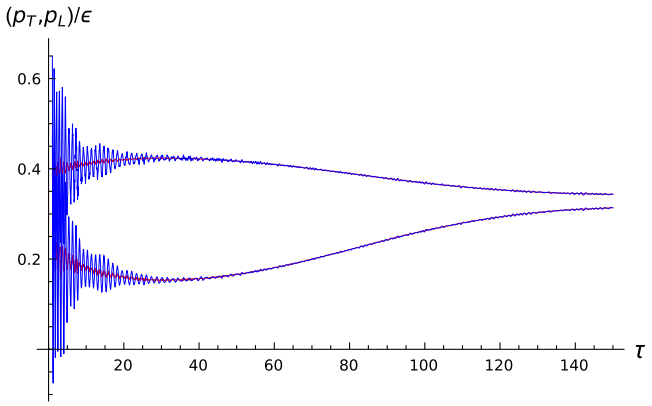

FIG. 4. The normalized transverse and longitudinal pressures for the canonical EMT (blue) and the conformal EMT (red). The initialization is $(\varphi_0, A) = (15, 0)$ and $k_x = k_y = 0.41$. The upper and lower lines are respectively $p_T/\mathcal{E}$ and $p_L/\mathcal{E}$.

and conformal EMTs. The blue curves show the oscillations that are characteristic of the canonical EMT, which die off at larger times when the decoherence terms $\sim\phi\dot{\phi}$ go to zero. The red curves are the results from the conformal EMT and are much smoother at early times. At $\tau \gtrsim 40$ the results from the two EMTs are indistinguishable.

We comment that if the curves in Figs. 3 and 4 were extended to longer times the transverse and longitudinal pressures would start to move away from each other. This happens because we work numerically with a box of finite size in coordinate space. The calculation breaks down at large times because there will be highly occupied momentum modes that are not supported. It has been shown that the transverse and longitudinal pressures become equal to each other at $\tau \approx 250$ if the number of grid points in the rapidity dimension is greater than about 160 [6].

C. Azimuthal asymmetry

When we use an initialization with $A \neq 0$ the initial fields are azimuthally asymmetric. We want to study how the azimuthal asymmetry of the energy density and momentum distribution develop in time, and how they are related to each other. Asymmetries in the transverse plane are orders of magnitude smaller than the transverse-longitudinal asymmetry discussed in the previous subsection, and they die out at very short times. As explained in Sec. I, the fact that these asymmetries disappear at very early times is part of the reason they are interesting. The maximum time that can be considered is limited by the value of N, as explained in Sec. V B. In all other calculations we have used $N = 121$ which allows us to consider times as large as 140 (lattice units). In the study of azimuthal symmetries, large times are not interesting and we therefore reduce the size of the lattice. In this section we use $(N, L, N_\gamma) = (81, 31, 256)$.

In Fig. 5 we show the eccentricity (left panel) and elliptic flow coefficient (right panel) as functions of τ for initializations $(\varphi_0, A, k_x) = (15, 1, 1.47)$ and $k_y \in (1.12, 1.30, 1.47)$.

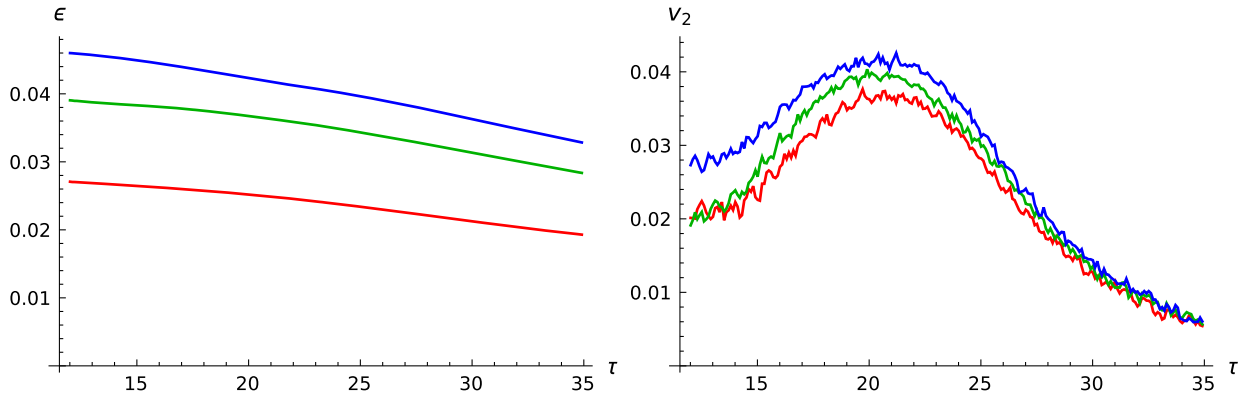

FIG. 5. The left panel shows the eccentricity as a function of τ and the right panel is the elliptic flow coefficient v_2. The initialization is $(\varphi_0, A, k_x) = (15, 1, 1.47)$ and from bottom to top $k_y = (1.12\,(\text{red}), 1.30\,(\text{green}), 1.47\,(\text{blue}))$.

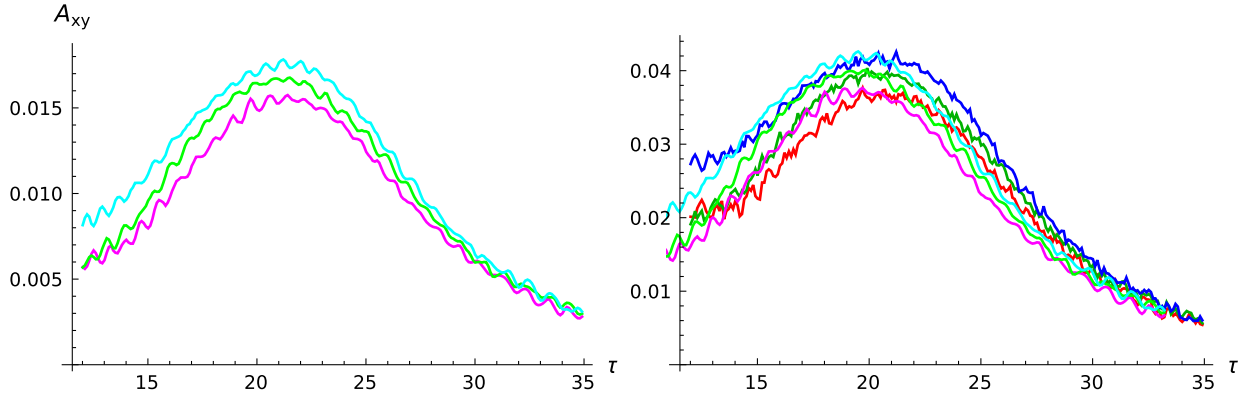

FIG. 6. The left panel is the transverse pressure asymmetry in Eq. (37) for the same initializations as in Fig. 5. The right panel is v_2 superimposed on a plot of A_{xy} that has been shifted left 1.7 time units and multiplied by a factor of 2.4. The lighter colored lines show the shifted results for A_{xy}.

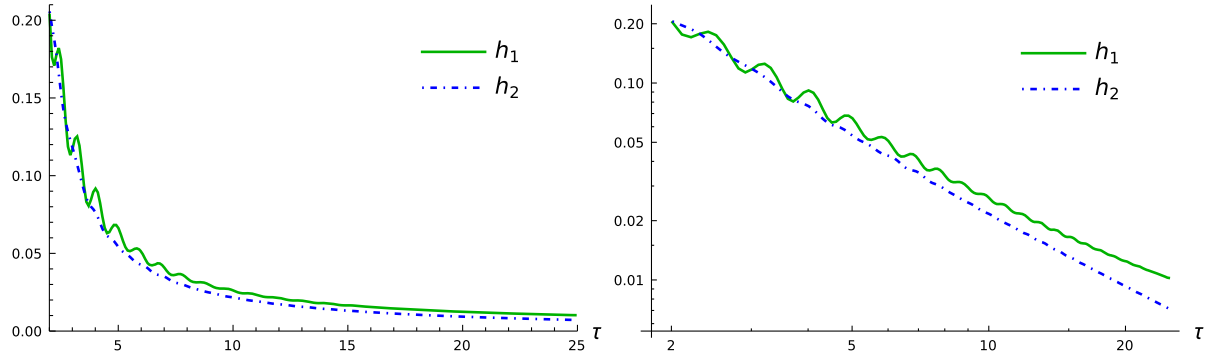

FIG. 7. The two quantities in Eq. (53) at early times. The left panel is a linear plot and the right is a log-log graph that shows the differences at later times more clearly. The calculation is done with $(\varphi_0, A) = (15, 0)$ and $k_x = k_y = 0.41$.

One sees that the initial spatial eccentricity decreases with time, and that the size of the initial eccentricity is correlated with the size of the momentum anisotropy that is produced. The elliptic flow coefficient initially increases and eventually decays. This behavior is characteristic of a hydrodynamic system in which pressure gradients are converted into fluid velocities, so that spatial anisotropy decreases and momentum anisotropy is generated. In Fig. 6 we show the similarity in the shape of the two measures v_2 and A_{xy} defined in Eqs. (36) and (37). The left panel shows A_{xy} for the same three initializations as in Fig. 5. The right panel shows the elliptic flow coefficient, and the transverse pressure asymmetry is shifted left by 1.7 time units and multiplied by 2.4 to help the reader to visually compare the two quantities. The similarity between the two graphs is another example of hydrodynamiclike features that emerge at very early times.

D. Universal flow

We can check how well Eq. (45) is satisfied for our system of scalar fields. The calculation is numerically difficult because the functions on both sides of the equation fluctuate in the transverse position at early times and decay rapidly as time increases. To compare them we calculate the root of the average of the squares of both sides of the equation. We define

$$h_1 = \sqrt{\left\langle \left(\frac{\tau}{2} \frac{\partial T^{00}}{\partial x} \right)^2 \right\rangle} \quad \text{and} \quad h_2 = \sqrt{\langle (T^{0x})^2 \rangle} \tag{53}$$

where the angle brackets indicate an average over spatial rapidity and the transverse coordinates.[9] Figure 7 shows there is good agreement of the two quantities in (53) at early times.

VI. CONCLUSIONS

In this paper we have studied the dynamics of a self-interacting real scalar field. We work with a conformally invariant action and calculate the energy-momentum tensor using the classical statistical approximation. We have

[9]The factor τ in h_1 is multiplied by the length scale $1/L$ because we have set the lattice spacing in the transverse direction to one.

studied the time evolution of the azimuthal asymmetry of the energy density and the momentum field and shown that the two quantities are correlated. The eccentricity decreases and the momentum elliptic flow coefficient initially increases and then later decays. We have studied the asymmetry of the transverse pressures and shown that its behavior is strikingly similar to that of the elliptic flow coefficient. Both of these behaviors are seen in hydrodynamic calculations that describe the physics of a relativistic heavy ion collision at much later times. We have compared the derivative of the transverse velocity and the gradient of the energy density and shown that the characteristics of universal flow are present in our system.

Our results provide further support for the use of the classical statistical approximation to describe a system of strongly coupled fields and suggest that the method is worthy of further investigation using more realistic initial configurations, and physical theories that involve additional fields. Such calculations could lead to a deeper understanding of the early onset of hydrodynamic behavior that is seen in heavy ion collisions.

ACKNOWLEDGMENTS

M. E. C. gratefully acknowledges helpful discussions with François Gelis. This work has been supported by the Natural Sciences and Engineering Research Council of Canada Discovery Grant program from Grants No. 2023-00023 and No. 2018-04090. This research was enabled in part by support provided by WestGrid [22] and the Digital Research Alliance of Canada [23].

APPENDIX: USEFUL EQUATIONS

In Milne coordinates the only nonzero components of the connection are $\Gamma^0_{\eta\eta} = \tau$ and $\Gamma^\eta_{0\eta} = \Gamma^\eta_{\eta 0} = 1/\tau$. The transformation from Minkowski to Milne coordinates is

$$A^\mu{}_\nu \equiv \frac{\partial x^\mu}{\partial x^\nu} = \begin{bmatrix} \cosh\eta & -\sinh(\eta) & 0 & 0 \\ -\frac{1}{\tau}\sinh(\eta) & \frac{1}{\tau}\cosh(\eta) & 0 & 0 \\ 0 & 0 & -1 & 0 \\ 0 & 0 & 0 & -1 \end{bmatrix}. \quad \text{(A1)}$$

Some results for the gradient operator are

$$\begin{aligned} \partial_\mu &= (\partial_\tau, \partial_\eta, \vec{\nabla}) \\ \partial^\mu &= \left(\partial_\tau, -\frac{1}{\tau^2}\partial_\eta, -\vec{\nabla}\right) \\ (\partial_\mu\varphi)(\partial^\mu\varphi) &= \dot{\varphi}^2 - \frac{1}{\tau^2}(\partial_\eta\varphi)^2 - (\vec{\nabla}\varphi)^2 \\ \Box &= \partial_\tau^2 + \frac{1}{\tau}\partial_\tau - \frac{1}{\tau^2}\partial_\eta^2 - \vec{\nabla}^2. \end{aligned} \quad \text{(A2)}$$

In Eqs. (A3) and (A4) we give the components of the canonical EMT (3) and the additional piece that appears in the conformal EMT (12). For the diagonal terms we give two ways to write the components of $T^{\mu\nu}_{\rm ex}$. The label "alt" indicates that the equation of motion has been used. These expressions are easier to calculate numerically. The components of the canonical EMT are

$$\begin{aligned} T^{00}_{\rm can} &= \frac{1}{2}\left((\dot{\phi})^2 + \frac{(\partial_\eta\phi)^2}{\tau^2} + (\partial_x\phi)^2 + (\partial_y\phi)^2\right) + \frac{g^2}{4!}\phi^4 \\ T^{\eta\eta}_{\rm can} &= \frac{1}{2}\tau^{-4}(\partial_\eta\phi)^2 + \frac{1}{\tau^2}\left[\frac{1}{2}((\dot{\phi})^2 - (\partial_x\phi)^2 - (\partial_y\phi)^2) - \frac{g^2}{4!}\phi^4\right] \\ T^{xx}_{\rm can} &= \left[\frac{1}{2}\left((\dot{\phi})^2 - \frac{(\partial_\eta\phi)^2}{\tau^2} + (\partial_x\phi)^2 - (\partial_y\phi)^2\right) - \frac{g^2}{4!}\phi^4\right] \\ T^{yy}_{\rm can} &= \left[\frac{1}{2}\left((\dot{\phi})^2 - \frac{(\partial_\eta\phi)^2}{\tau^2} - (\partial_x\phi)^2 + (\partial_y\phi)^2\right) - \frac{\lambda}{4!}\phi^4\right] \\ T^{xy}_{\rm can} &= (\partial_x\phi)(\partial_y\phi) \\ T^{0\eta}_{\rm can} &= -\frac{1}{\tau^2}\dot{\phi}(\partial_\eta\phi) \\ T^{0y}_{\rm can} &= -\dot{\phi}(\partial_y\phi) \\ T^{0x}_{\rm can} &= -\dot{\phi}(\partial_x\phi). \end{aligned} \quad \text{(A3)}$$

The components of $T^{\mu\nu}_{\rm ex}$ are

$$
\begin{aligned}
T^{00}_{\mathrm{ex}} &= \frac{1}{3}\frac{1}{\tau}(\varphi\dot{\varphi}) - \frac{1}{3}\frac{1}{\tau^2}((\partial_\eta\varphi)^2 + \varphi\partial_\eta^2\varphi) - \frac{1}{3}\vec{\nabla}_\perp\cdot(\varphi\vec{\nabla}_\perp\varphi)\\
T^{00}_{\mathrm{ex-alt}} &= -\frac{1}{3}\left[\phi\ddot{\phi} + \frac{g^2}{6}\phi^4 + \frac{(\partial_\eta\phi)^2}{\tau^2} + |\nabla_\perp\phi|^2\right]\\
T^{\eta\eta}_{\mathrm{ex}} &= -\frac{1}{3\tau^2}\frac{\partial}{\partial\tau}(\varphi\dot{\varphi}) + \frac{1}{3\tau^2}\vec{\nabla}_\perp\cdot(\varphi\vec{\nabla}_\perp\varphi)\\
T^{\eta\eta}_{\mathrm{ex-alt}} &= -\frac{1}{3\tau^4}\left[\phi\partial_\eta^2\phi - \tau\phi\dot{\phi} - \frac{g^2}{6}\phi^4\tau^2 + \tau^2(\dot{\phi}^2 - |\nabla_\perp\phi|^2)\right]\\
T^{xx}_{\mathrm{ex}} &= -\frac{1}{3}\left(\frac{\partial}{\partial\tau}(\varphi\dot{\varphi}) + \frac{1}{\tau}(\varphi\dot{\varphi}) - \frac{1}{\tau^2}\partial_\eta(\varphi\partial_\eta\varphi)\right) + \frac{1}{3}\frac{\partial}{\partial y}\left(\phi\frac{\partial\phi}{\partial y}\right)\\
T^{xx}_{\mathrm{ex-alt}} &= -\frac{1}{3}\left[\phi\partial_x^2\phi - \frac{g^2}{6}\phi^4 + (\dot{\phi})^2 - \frac{(\partial_\eta\phi)^2}{\tau^2} - (\partial_y\phi)^2\right]\\
T^{yy}_{\mathrm{ex}} &= -\frac{1}{3}\left(\frac{\partial}{\partial\tau}(\varphi\dot{\varphi}) + \frac{1}{\tau}(\varphi\dot{\varphi}) - \frac{1}{\tau^2}\partial_\eta(\varphi\partial_\eta\varphi)\right) + \frac{1}{3}\frac{\partial}{\partial x}\left(\phi\frac{\partial\phi}{\partial x}\right)\\
T^{yy}_{\mathrm{ex-alt}} &= -\frac{1}{3}\left[\phi\partial_y^2\phi - \frac{g^2}{6}\phi^4 + (\dot{\phi})^2 - \frac{(\partial_\eta\phi)^2}{\tau^2} - (\partial_x\phi)^2\right]\\
T^{0\eta}_{\mathrm{ex}} &= \frac{1}{3\tau^2}\left(\phi\partial_\eta\dot{\phi} + \dot{\phi}\partial_\eta\phi - \frac{1}{\tau}\phi\partial_\eta\phi\right)\\
T^{0x}_{\mathrm{ex}} &= \frac{1}{3}(\phi\partial_x\dot{\phi} + \dot{\phi}\partial_x\phi)\\
T^{0y}_{\mathrm{ex}} &= \frac{1}{3}(\phi\partial_y\dot{\phi} + \dot{\phi}\partial_y\phi)\\
T^{xy}_{\mathrm{ex}} &= -\frac{1}{3}[\phi(\partial_x\partial_y\phi) + (\partial_x\phi)(\partial_y\phi)].
\end{aligned}
\tag{A4}
$$

[1] S. Schlichting and D. Teaney, Annu. Rev. Nucl. Part. Sci. **69**, 447 (2019).
[2] J. Berges, M. P. Heller, A. Mazeliauskas, and R. Venugopalan, Rev. Mod. Phys. **93**, 035003 (2021).
[3] K. Rajagopal, B. Scheihing-Hitschfeld, and R. Steinhorst, arXiv:2405.17545.
[4] K. Dusling, T. Epelbaum, F. Gelis, and R. Venugopalan, Nucl. Phys. **A850**, 69 (2011).
[5] T. Epelbaum and F. Gelis, Nucl. Phys. **A872**, 210 (2011).
[6] K. Dusling, T. Epelbaum, F. Gelis, and R. Venugopalan, Phys. Rev. D **86**, 085040 (2012).
[7] T. Epelbaum and F. Gelis, Phys. Rev. Lett. **111**, 232301 (2013).
[8] M. E. Carrington, G. Kunstatter, C. D. Phillips, and M. E. Rubio, Entropy **24**, 1612 (2022).
[9] J. Berges, K. Boguslavski, S. Schlichting, and R. Venugopalan, J. High Energy Phys. 05 (2014) 054.
[10] T. Epelbaum, F. Gelis, and B. Wu, Phys. Rev. D **90**, 065029 (2014).
[11] F. Gelis and S. Hauksson, arXiv:2403.11908.
[12] J. Vredevoogd and S. Pratt, Phys. Rev. C **79**, 044915 (2009).
[13] D. N. Blaschke, F. Gieres, M. Reboud, and M. Schweda, Nucl. Phys. **B912**, 192 (2016).
[14] Leonard Parker and David Toms, *Quantum Field Theory in Curved Spacetime* (Cambridge University Press, Cambridge, England, 2009).
[15] S. A. Voloshin, A. M. Poskanzer, and R. Snellings, Landolt-Bornstein **23**, 293 (2010).
[16] U. Heinz and R. Snellings, Annu. Rev. Nucl. Part. Sci. **63**, 123 (2013).

[17] P. F. Kolb, J. Sollfrank, and U. W. Heinz, Phys. Lett. B **459**, 667 (1999).
[18] J. P. Blaizot, W. Broniowski, and J. Y. Ollitrault, Phys. Lett. B **738**, 166 (2014).
[19] M. E. Carrington, A. Czajka, and S. Mrówczyński, Phys. Rev. C **106**, 034904 (2022).
[20] M. Luzum and P. Romatschke, Phys. Rev. C **78**, 034915 (2008).
[21] M. Luzum and P. Romatschke, Phys. Rev. Lett. **103**, 262302 (2009).
[22] www.westgrid.ca
[23] alliancecan.ca